Influence of surface tension on fractal contact model

Article *in* Journal of Applied Physics · February 2014

DOI: 10.1063/1.4869742

Influence of surface tension on fractal contact model

J. M. Long, G. F. Wang, X. Q. Feng, and S. W. Yu

Citation: Journal of Applied Physics **115**, 123522 (2014); doi: 10.1063/1.4869742
View online: https://doi.org/10.1063/1.4869742
View Table of Contents: http://aip.scitation.org/toc/jap/115/12
Published by the American Institute of Physics

Influence of surface tension on fractal contact model

J. M. Long,[1] G. F. Wang,[1,a)] X. Q. Feng,[2] and S. W. Yu[2]
[1]*Department of Engineering Mechanics, SVL, Xi'an Jiaotong University, Xi'an 710049, China*
[2]*Department of Engineering Mechanics, AML, Tsinghua University, Beijing 100084, China*

(Received 20 January 2014; accepted 16 March 2014; published online 28 March 2014)

Almost all solid surfaces have roughness on different length scales, from macro, micro to nano. In the conventional fractal contact model, the macroscopic Hertzian contact theory is employed to predict the contact load-area relation for all sizes of contact spots. However, when the contact radius of an asperity shrinks to nanometers, surface tension may greatly alter the contact behavior. In the present paper, we address surface effects on the contact between a rigid sphere and an elastic half space, and we demonstrate that the contact load-area relation is size-dependent, especially for nanosized asperities. Then, the refined contact relation is incorporated into the Majumdar-Bhushan fractal contact model. It is found that the presence of surface tension requires higher load than the conventional fractal contact model to generate the same real contact area.
[http://dx.doi.org/10.1063/1.4869742]

I. INTRODUCTION

Almost all surfaces of solids are rough, if observed at micro and nanoscales. The contact of rough surfaces is of crucial importance in friction, wear, and lubrication. Usually, a rough surface can be characterized by statistical parameters such as the standard deviations of surface heights, slopes and curvatures,[1] and corresponding elastic and plastic contact models have been developed.[2,3] However, it is noticed that the variances of slopes and curvatures of a rough surface depend strongly on the resolution of roughness-measuring instrument, and the variance of height distribution is related to the dimensions of the statistical samples.[4,5] Therefore, for a specific pair of rough surfaces, these contact models may not give a unique prediction.

Alternatively, many natural surfaces can be described by self-affine fractal geometry.[6] Using the Weierstrass-Mandelbrot function[7] to characterize self-affine fractal surface, Majumdar and Bhushan[8] and Yan and Komvopoulos[9] studied the elastic-plastic contact between two rough surfaces. Through molecular dynamics simulations, Yang *et al.*[10] investigated the contact of a liquid droplet on a self-affine fractal surface. Pohrt and Popov[11] calculated the normal interfacial stiffness of two elastic bodies with randomly rough surfaces and varying fractal dimensions.

If a self-affine fractal surface is repeatedly magnified, more details of roughness can be observed at finer length scales, as shown in Fig. 1. Through an optical interferometer with 1 μm resolution and a scanning tunneling microscope with 1 nm resolution, roughness was observed at both millimeter and nanometer scales.[8] Recently, both experiments and atomic simulations demonstrate that nanomaterials and nanosized structural elements may have distinctly different mechanical properties from their macroscopic counterparts.[12,13] Size-dependent characteristics at nanoscale can be attributed to the effects of surface energy or surface tension, which are not included in classical continuum mechanics.[14–17] Based on the surface elasticity theory, He and Lim[18] and Huang and Yu[19] derived the surface Green function for three- and two-dimensional problems, respectively. Chen and Zhang[20] presented the analytical Green's functions for anti-plane shear deformation. For nanoindentation, Long and Wang[21] revealed that surface tension may significantly alter the pressure distribution under the indenter, and they predicted a size-dependent hardness.

Majumdar-Bhushan model is the most widely used fractal contact model. It uses the conventional Hertzian contact theory to describe the load-area relation across all length scales spanning from the sample size to infinitesimal.[8] When the characteristic length of contact spots reduces to nanometers, it would be necessary to account for surface effects. In the present paper, we will develop a new self-affine fractal contact model with the effects of surface tension.

The paper is organized as follows. In Sec. II, Majumdar-Bhushan fractal contact model (MB model) is briefly reviewed. The influence of surface tension on nanosized contact problems will be formulated in Sec. III. Then the obtained load-area relation for nanosized contact spot will be incorporated into the MB model in Sec. IV.

II. MAJUMDAR-BHUSHAN FRACTAL CONTACT MODEL

First, we briefly review the MB model, and its more details can be found in Ref. 8. Consider the contact between an isotropic self-affine fractal rough surface and a flat plane, as shown in Fig. 1. The contact spots have stochastic sizes and are randomly distributed over the contact interface. Specify a contact spot with area a, and then its characteristic length can be estimated by $l = a^{1/2}$.

Using the Weierstrass-Mandelbrot function,[7] the roughness is assumed as a cosinusoidal wave, as shown in Fig. 1(c). For a wavelength of l, the asperity shape is described as

$$z(x) = W^{D-1} l^{2-D} \cos\left(\frac{\pi x}{l}\right), \quad \left(-\frac{l}{2} < x < \frac{l}{2}\right), \qquad (1)$$

[a)]Author to whom correspondence should be addressed. Electronic mail: wanggf@mail.xjtu.edu.cn

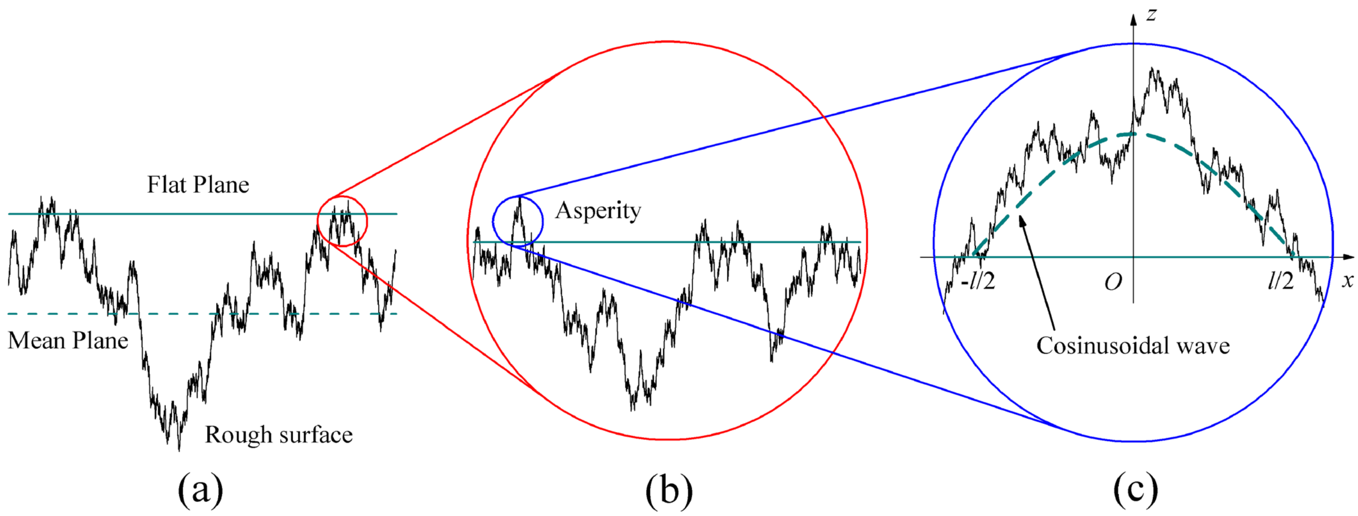

FIG. 1. Contact between a self-affine fractal rough surface and a flat plane.

where W is the fractal roughness parameter, and D is the fractal dimension to be determined from the power spectrum of the Weierstrass-Mandelbrot function.

The radius of curvature R at the tip of the asperity is given by

$$R = \left| \left(\frac{d^2 z}{dx^2}\Big|_{x=0} \right)^{-1} \right| = \frac{a^{D/2}}{\pi^2 W^{D-1}}. \tag{2}$$

In the MB model, the critical area of contact spot demarcating the elastic and plastic regimes is determined by

$$a_c = \frac{W^2}{(B\phi/2)^{2/(D-1)}}, \tag{3}$$

where $\phi = \sigma_y/E^*$ is a dimensionless material parameter, σ_y is the yield strength, and E^* is the composite elastic modulus. B is a factor defined as the ratio between the hardness H and the yield stress σ_y, that is, $H = B\sigma_y$.

When the contact area of a spot is larger than the critical area ($a > a_c$), the spot will undergo purely elastic deformation and the contact force P_e acting on this spot is given by the linear elastic Hertzian theory as[22]

$$P_e(a) = \frac{4E^* a^{3/2}}{3\pi^{3/2} R}. \tag{4}$$

Substitution of Eq. (2) into (4) gives

$$P_e(a) = \frac{4\sqrt{\pi}}{3} E^* W^{D-1} a^{(3-D)/2}. \tag{5}$$

When the contact area of a spot is smaller than the critical area ($a < a_c$), the spot falls into the plastic regime, and the contact force P_p on this spot is written as

$$P_p(a) = B\sigma_y a. \tag{6}$$

Denote the size-distribution of contact spots by $n(a)$. Then, the total contact load is calculated by

$$P = \int_{a_c}^{a_l} P_e(a) n(a) da + \int_0^{a_c} P_p(a) n(a) da, \tag{7}$$

where a_l is the largest contact area among all spots.

Following the geomorphology analysis in Ref. 23, Majumdar and Bhushan[8] assumed that the sizes of contact spots follow a power law distribution:

$$n(a) = \frac{D}{2} \frac{a_l^{D/2}}{a^{D/2+1}}. \tag{8}$$

In this case, the real contact area is

$$A_r = \int_0^{a_l} n(a) a da = \frac{D}{2-D} a_l. \tag{9}$$

By substituting Eqs. (5) and (6) into Eq. (7), the nondimensional total contact load is determined as (for $D \neq 1.5$),

$$\begin{aligned} P^* = {} & \frac{4\sqrt{\pi}}{3} W^{*(D-1)} \frac{D}{3-2D} \left(\frac{2-D}{D}\right)^{D/2} A_r^{*D/2} \\ & \times \left[\left(\frac{2-D}{D} A_r^* \right)^{\frac{3-2D}{2}} - (a_c^*)^{\frac{3-2D}{2}} \right] \\ & + K\phi \left(\frac{D}{2-D} \right)^{(2-D)/2} A_r^{*D/2} a_c^{*(2-D)/2}, \end{aligned} \tag{10}$$

where

$$P^* = \frac{P}{A_a E^*}, \quad W^* = \frac{W}{\sqrt{A_a}}, \quad A_r^* = \frac{A_r}{A_a},$$
$$a_c^* = \frac{a_c}{A_a} = \frac{W^{*2}}{(K\phi/2)^{2/(D-1)}},$$

A_a is the apparent contact area. For $D = 1.5$, the nondimensional total load is expressed as

$$P^* = \sqrt{\pi} W^{*1/2} \left(\frac{A_r^*}{3} \right)^{3/4} \ln\left(\frac{A_r^*}{3a_c^*} \right) + 3B\phi \left(\frac{A_r^*}{3} \right)^{3/4} a_c^{*1/4}. \tag{11}$$

For a surface fabricated from polyester-polyurethane,[24] Bhushan obtained the material constants $D = 1.49$, $B\phi = 0.1$, and the fractal roughness parameter $W = 1 \times 10^{-13}$ m. According to Eq. (3), the critical area a_c is 2.04×10^{-21} m^2, indicating that most contact spots will be in the elastic regime. The nominal contact area A_a of the sample is 1 mm^2. If the ratio of real contact area to nominal area is set as 0.1, A_r will be 10^{-7} m^2 and Eq. (9) predicts the largest contact area $a_l = 3.43 \times 10^{-8}$ m^2. It is found that the contact radii of asperities span from microns to nanometers for the considered surface. Therefore, surface effects should be considered in the elastic contact problem between two rough surfaces.

III. HERTZIAN CONTACT MODEL WITH SURFACE EFFECTS

Surface stress or surface energy often plays an important role in the mechanical behavior of solids at nanoscale. The presence of surface stress gives rise to a non-classical boundary condition. In the presence of surface stresses, the equilibrium conditions on a surface becomes[25,26]

$$t_\alpha + \sigma^s_{\beta\alpha,\beta} = 0, \tag{12}$$

$$\sigma_{ij} n_i n_j = \sigma^s_{\alpha\beta} \kappa_{\alpha\beta}, \tag{13}$$

where t_α denotes the surface traction in the x_α-direction, n_i the unit vector normal to the surface, $\kappa_{\alpha\beta}$ the curvature tensor of the surface, and $\sigma^s_{\alpha\beta}$ the surface stress tensor. Einstein's summation convention is adopted for repeated Latin indices (1, 2, 3) and Greek indices (1, 2).

The surface stress tensor $\sigma^s_{\alpha\beta}$ is related to surface energy density $\gamma(\varepsilon_{\alpha\beta})$ by[27]

$$\sigma^s_{\alpha\beta} = \gamma \delta_{\alpha\beta} + \frac{\partial \gamma}{\partial \varepsilon_{\alpha\beta}}. \tag{14}$$

If the change of the atomic spacing in the surface layer during deformation is infinitesimal, the contribution from the second term to surface stress will be negligible. Thus, the surface stresses will be constant and expressed as

$$\sigma^s_{\alpha\beta} = \gamma \delta_{\alpha\beta}. \tag{15}$$

Now we formulate the three-dimensional contact problem with the influence of surface tension. Consider a rigid sphere with radius R indenting on an isotropic elastic half space, as shown in Fig. 2. Refer to the Cartesian coordinate system (O-xyz), where the origin O is located at the initial contact point, the x-axis along the initial surface of the half space, and the z-axis perpendicular to the surface. A vertical resultant force P_{es} is applied on the sphere along the z-direction. The induced indentation depth is designated as δ, and the radius of the corresponding circular contact region is b. In the case of small deformation, the boundary condition in the contract region is described by

$$w(r,0) = \delta - \left(R - \sqrt{R^2 - r^2}\right) \approx \delta - \frac{r^2}{2R}, \quad \text{for } r \le b, \tag{16}$$

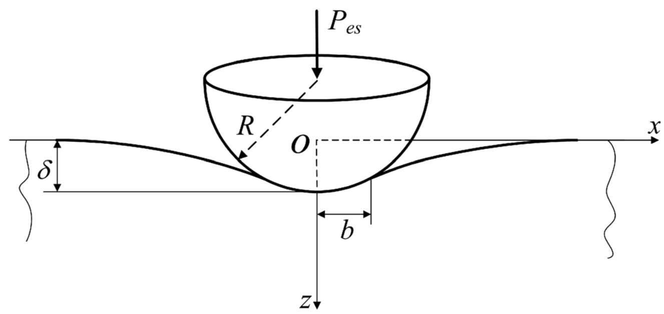

FIG. 2. Indentation of a rigid sphere on an elastic half space.

where $w(r,0)$ is the normal displacement of the surface and $r^2 = x^2 + y^2$.

When surface tension is taken into account, the boundary condition in Eq. (13) outside the contact region is written as

$$\sigma_{33}(r,0) = \gamma \frac{\mathrm{d}}{r\mathrm{d}r}\left[r \frac{\mathrm{d}w(r,0)}{\mathrm{d}r}\right], \quad \text{for} \quad r > b, \tag{17}$$

where $\sigma_{33}(r,0)$ is the normal stress in the bulk material on the surface.

Under the assumption of frictionless contact, the tangential stress on the whole upper surface of the half space is negligible, that is,

$$\sigma_{13}(r,0) = 0. \tag{18}$$

For a point force L acting on a surface with surface tension, the normal displacement on the contact surface is presented as[28]

$$w(r,0) = \frac{L}{4\gamma}\left[H_0\left(\frac{r}{s}\right) - Y_0\left(\frac{r}{s}\right)\right], \tag{19}$$

where $s = 2\gamma / E^*$ is an intrinsic material length indicating the relative significance of surface tension, H_0 and Y_0 are the zero-order Struve function and the zero-order Bessel function of the second kind, respectively. We denote the axisymmetric pressure distribution as $p(t)$. Then the normal displacement of the surface caused by the pressure acting on the whole contact region can be expressed as

$$w(r,0) = \int_0^{2\pi}\int_0^b \left[H_0\left(\frac{k}{s}\right) - Y_0\left(\frac{k}{s}\right)\right]\frac{p(t)t}{4\gamma}\,\mathrm{d}\theta\,\mathrm{d}t, \tag{20}$$

where $k^2 = r^2 + t^2 - 2rt\cos\theta$. Substitution of Eq. (20) into (16) leads to

$$\frac{1}{2\gamma}\int_0^b\int_0^\pi \left[H_0\left(\frac{k}{s}\right) - Y_0\left(\frac{k}{s}\right)\right] tp(t)\,\mathrm{d}t\mathrm{d}\theta = \delta - \frac{r^2}{2R}. \tag{21}$$

Differentiating Eq. (21) with respect to r, one has

$$\frac{1}{2\gamma s}\int_0^b\int_0^\pi \left[H_1\left(\frac{k}{s}\right) - \frac{2}{\pi} - Y_1\left(\frac{k}{s}\right)\right]\frac{r - t\cos\theta}{k} tp(t)\,\mathrm{d}t\mathrm{d}\theta = \frac{r}{R}, \tag{22}$$

where H_1 and Y_1 are the first-order Struve function and the first-order Bessel function of the second kind, respectively. Since the resultant pressure over the contact region equals the external loading P_{es}, we have

$$\int_0^{2\pi}\int_0^b p(t)t\mathrm{d}\theta\mathrm{d}t = 2\pi\int_0^b tp(t)\mathrm{d}t = P_{es}. \tag{23}$$

Invoking the Gauss-Chebyshev quadrature formula, one can use a numerical method to solve the singular integral equation (22), in conjunction with its constraint condition in Eq. (23).[29] Then the total contact load P_{es} can be derived as a function of the contact radius b or the contact area a.

For the considered polyester-polyurethane surface, the composite elastic modulus is $E^* = 1804\,\mathrm{MPa}$.[24] The surface energy density γ of the material is not available in the literature, but usually it is on the order of 1 J/m^2. For a representative value of $\gamma = 0.4\,\mathrm{J/m^2}$, Fig. 3 displays the relation between the normalized load P_{es} and the normalized contact area a for different radii of indenters. According to the classical Hertzian contact model (Eq. (4)), the normalized P_{es} versus a curve will be independent of the indenter radius. However, when surface tension is taken into account, the $P_{es} - a$ relation depends clearly on the indenter size. When the indenter radius is larger than 10 μm, the influence of surface tension is negligible and the present model reduces to the classical Hertzian solution. However, as the indenter radius reduces to nanometers, surface tension evidently alters the contact load-area curve. Since surface tension sustains a part of external loading, a higher load is required to generate the same contact area compared with the classical Hertzian model. The smaller the indenter radius, the more significant the effect of surface tension.

IV. MB MODEL WITH SURFACE EFFECTS

In the MB fractal contact model described in Sec. II, the contact areas of spots under elastic deformation range from a_c to a_l. For smaller spots in this range, surface tension may distinctly alter the contact load-area relation, as shown in Sec. III. Moreover, with the increase in the fractal dimension D, the contribution of small sized spots to the total contact area will become more prominent. For example, for $D = 1.9$, more than 50% of the total contact area results from those spots with contact area smaller than $10^{-6}a_l$.[8] For nanosized contact, therefore, the contact load–area relation in conventional fractal contact model Eqs. (4) or (5) should be modified to account for the influence of surface tension.

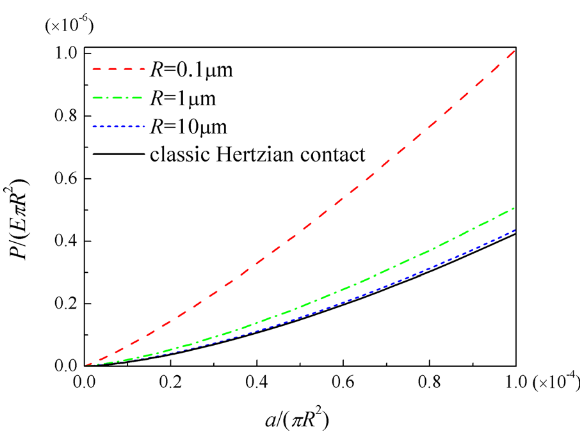

FIG. 3. Normalized contact load-area relation of a rigid sphere in contact with an elastic half space.

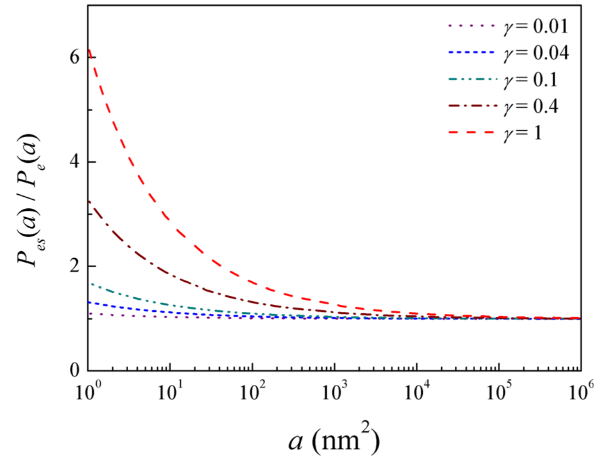

FIG. 4. Variation of the contact load with respect to the contact area of spot.

For a self-affine fractal rough surface, the curvature radius R of a contact spot depends on the contact area a, as given in Eq. (2). Then using the method in Sec. III, we can determine the corresponding load P_{es} on this spot. For various values of surface tension, Fig. 4 demonstrates the variation of normalized contact load P_{es} normalized by P_e in Eq. (5) with respect to a. It is obvious that surface tension tends to enlarge the contact load in the range of nanosized contact area. The larger the surface tension, the higher the required load, and the wider the affected domain of contact area.

Then the total load is given by

$$P_s = \int_{a_c}^{a_l} P_{es}(a)n(a)\mathrm{d}a + \int_0^{a_c} P_p(a)n(a)\mathrm{d}a. \tag{24}$$

From Eq. (24), together with Eqs. (6) and (8), we can obtain the total contact load with the influence of surface tension. Fig. 5 displays the relation between the normalized total load and the real contact area for the polyester-polyurethane system. When surface tension is small (i.e., 0.01 J/m^2), the

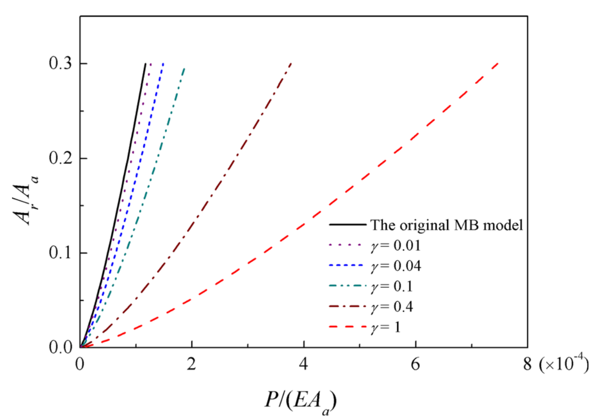

FIG. 5. Relation between the total contact load and the real contact area.

contribution of surface tension is negligible and the present model is close to the MB model. However, as the surface tension increases, a larger load is required to yield the same real contact area than the MB model. For a specific surface with a fixed surface tension, the contribution of surface tension to the contact load also increases with increasing real contact area. As the load gets even larger, the plastic deformation and the interaction between neighboring asperities might become important,[30] which are interesting issues and deserve further research.

V. CONCLUSIONS

For self-affine fractal rough surfaces in contact, the contact radii of spots may span from microns to nanometers. In the present paper, the influence of surface tension in nanosized contact problem has been examined by considering the contact between a rigid sphere and an elastic half space. The results reveal that the contact load-area relation is size-dependent for nanoindentation. Then, in the conventional fractal contact model (MB model), we incorporate the refined relation between contact load and area with surface effects. For a specific real contact area, the new model predicts a higher contact load than the original MB model. This study is helpful to understand the micro-contact between rough surfaces.

ACKNOWLEDGMENTS

Supports from the National Natural Science Foundation of China (11272249 and 11021202), 973 Program of MOST (2010CB631005), and the Scholarship Award for Excellent Doctoral Student granted by the Education Ministry of China are acknowledged.

[1]P. R. Nayak, J. Lubr. Technol. **93**, 398 (1971).
[2]J. A. Greenwood and J. B. P. Williamson, Proc. R. Soc. Lond. Ser. A **295**, 300 (1966).
[3]P. R. Nayak, Wear **26**, 305 (1973).
[4]B. Bhushan, J. C. Wyant, and J. Meiling, Wear **122**, 301 (1988).
[5]R. S. Sayles and T. R. Thomas, Nature **271**, 431 (1978).
[6]J. Feder, *Fractals* (Plenum Press, New York, 1988).
[7]M. V. Berry and Z. V. Lewis, Proc. R. Soc. Lond. Ser. A **370**, 459 (1980).
[8]A. Majumdar and B. Bhushan, J. Tribol. **113**, 1 (1991).
[9]W. Yan and K. Komvopoulos, J. Appl. Phys. **84**, 3617 (1998).
[10]C. Yang, U. Tartaglino, and B. N. J. Persson, Phys. Rev. Lett. **97**, 116103 (2006).
[11]R. Pohrt and V. L. Popov, Phys. Rev. Lett. **108**, 104301 (2012).
[12]C. Q. Chen, Y. Shi, Y. S. Zhang, J. Zhu, and Y. J. Yan, Phys. Rev. Lett. **96**, 075505 (2006).
[13]R. E. Miller and V. B. Shenoy, Nanotechnology **11**, 139 (2000).
[14]H. L. Duan, J. Wang, Z. P. Huang, and B. L. Karihaloo, J. Mech. Phys. Solids **53**, 1574 (2005).
[15]W. Gao, S. W. Yu, and G. Y. Huang, Nanotechnology **17**, 1118 (2006).
[16]G. F. Wang and X. Q. Feng, Appl. Phys. Lett. **90**, 231904 (2007).
[17]C. Q. Ru, Appl. Phys. Lett. **94**, 051905 (2009).
[18]L. H. He and C. W. Lim, Int. J. Solids Struct. **43**, 132 (2006).
[19]G. Y. Huang and S. W. Yu, J. Appl. Mech. **74**, 821 (2007).
[20]W. Q. Chen and C. Zhang, Int. J. Solids Struct. **47**, 1641 (2010).
[21]J. M. Long and G. F. Wang, Mech. Mater. **56**, 65 (2013).
[22]K. L. Johnson, *Contact Mechanics* (Cambridge University Press, Cambridge, 1985).
[23]B. B. Mandelbrot, Proc. Nat. Acad. Sci. U.S.A. **72**, 3825 (1975).
[24]B. Bhushan, ASLE Trans. **28**, 181 (1985).
[25]M. E. Gurtin and A. I. Murdoch, Arch. Ration. Mech. Anal. **57**, 291 (1975).
[26]M. E. Gurtin, J. Weissmuller, and F. Larche, Philos. Mag. A **78**, 1093 (1998).
[27]R. C. Cammarata, Progr. Surf. Sci. **46**, 1 (1994)
[28]M. A. Hajji, J. Appl. Mech. **45**, 320 (1978).
[29]F. Erdogan and G. D. Gupta, Quart. Appl. Math. **29**, 525 (1972).
[30]J. Pullen and J. B. P. Williamson, Proc. R. Soc. Lond. Ser. A **327**, 159 (1972).